Journal of Applied Research and Technology

www.jart.icat.unam.mx

Journal of Applied Research and Technology 23 (2025) 145-154

Original

Optimal tuning of PID-type controllers

P. Teppa-Garran*[a] • G. Bohórquez[b] • G. Garcia[c]

[a]*Departamento de Gestión de Proyectos y Sistemas, Universidad Metropolitana, Caracas, Venezuela*
[b]*Escuela de Ingeniería Eléctrica, Universidad Metropolitana, Caracas, Venezuela*
[c]*CNRS, LAAS, 7 Avenue du Colonel Roche, Toulouse, France and Université de Toulouse, INSA, Toulouse, France*

Received 02 16 2024; accepted 10 04 2024
Available 04 30 2025

Abstract: Direct methods for optimal tuning of the parameters of a PID-type controller are developed using the theory of LQR when the order of the plant model equation is known. This is achieved through two fundamental results. The first one defines a link between the weighting matrix of the LQR performance index with the desired temporal specifications of the closed-loop controlled response, expressed through a desired overshoot and settling time, as well as the tracking of a constant reference input with zero steady-state error. The second result establishes the connection between the state feedback solution of the LQR problem and the parameters of the PID-type controller. The design method is validated through simulation studies on a heat flow experiment, a coupled tank system, and a radar antenna.

Keywords: PI, PID, PID^{n-1}, LQR, heat flow experiment, coupled tank system, radar antenna.

*Corresponding author.
E-mail address: pteppa@unimet.edu.ve (P. Teppa-Garran).
Peer Review under the responsibility of Universidad Nacional Autónoma de México.

1. Introduction

Proportional-integral (PI) and Proportional-Integral-Derivative (PID) controllers are the central control policies used in industry (Åström & Hagglund, 1995; Desborough & Miller, 2012). There are numerous rules for systematically tuning the parameters of these controllers, and much of this work has been done for linear systems in the time domain (Teppa-Garran et al., 2021). When it is considered that the plant is described by a mathematical model of a specific order, direct formulas can be obtained for tuning the parameters of the PI or PID controller: a first-order model for the case of PI and a second-order model for the PID. For a plant of order n, a PID-type controller (PID^{n-1}) is expressed as (Teppa-Garran & Garcia, 2013):

$$u(t) = K_p e(t) + K_i \int_0^t e(\tau)\, d\tau + K_{d_1}\dot{e}(t) + K_{d_2}\ddot{e}(t) + \cdots + K_{d_{n-1}} e^{(n-1)}(t) \tag{1}$$

This equation includes traditional PI and PID controllers when the order n of the system is one or two, respectively.

On the other hand, despite their widespread application, many poorly tuned PI and PID controllers are operating in the industry (Lee et al., 2014). The linear quadratic regulator (LQR) (Anderson & Moore, 2007; Lavretsky & Wise, 2013) is a well-known design technique in optimal control theory that has been studied for decades, and it has a simple, closed-form solution on the infinite time horizon case. In LQR, the desired performance objectives are addressed directly by minimizing a quadratic function of the state and the control input. The resulting optimal control law has many suitable properties, including closed-loop stability. Furthermore, by choosing the weighting matrices, it is possible to control the tradeoff between the requirements for regulating the state and the expenditure of control energy. However, a significant criticism is that the selection of the weighting matrices in the quadratic function needs to be clarified to meet the closed-loop design specifications (Teppa-Garran & Garcia, 2014). Even more, the connection to the closed-loop dynamics is indirect; it depends on the choice of the weighting matrices. Thus, one usually needs to perform some trial-and-error procedure to obtain a satisfactory closed-loop response.

The use of the method LQR for optimal tuning of the PID parameters has been applied previously. For example, (Argentim et al., 2013) employ an LQR loop to tune a PID on a quadcopter platform. A hybrid LQR-PID for seismic control of buildings is proposed in Heidari et al. (2018). In Anh (2020), a coordinate PID-LQR is used for an active suspension system; the PID part controls the body acceleration, and the LQR controls the body displacement. Finally, Choubey and Ohri (2022) propose a gray wolf optimizer to tune the PID parameters by selecting the weighting matrices of LQR for optimal path control of a 3-DOF Maryland manipulator. The objective and main contribution of this article is the construction of direct methods that allow optimal tuning of the parameters of a PID-type controller expressed as (1) employing the LQR formulation by incorporating time specifications of tracking, overshoot, and settling time in the closed-loop controlled output through the selection of the weighting matrices of the quadratic function. This idea has already been considered in Oral et al. (2010), where a method to translate the time requirements into the LQR quadratic function is proposed, but considering a state feedback control policy and restricted to the bridge crane model equations, also, in He et al. (2000), where the LQR method is employed to tune a PI controller for the first order plus time delay system. The method is extended to tune a PID but considering that the second-order system is overdamped, the derivative component of the controller is chosen to cancel the fast pole of the model, and in this way, the PI tuning method can still be applied. Our proposed PI tuning method for a first-order system follows the idea of (He et al., 2000). Still, as we do not consider time delay, the design procedure is more straightforward because the LQR problem is of infinite time, resulting in an algebraic Riccati equation. Additionally, to obtain the design equations, a zero-reference input (regulation problem) is not needed; the design is formulated to track any constant reference input. On the other hand, our proposed PID method works for a general second-order system; that is, there is no constraint in the search space for the parameters. Finally, design equations for general PID controllers for systems of higher order are developed. The methods are validated through different simulation studies.

Notation: $\dot{a}(t) = da/dt$, $\ddot{a}(t) = d^2a/dt^2$, $a^{(n)}(t) = d^n a/dt^n$ Capital bold typeface letters denote matrices and small bold typeface letter vectors. $\mathbb{R}$ is the set of real numbers.

2. Basic results

Consider the closed-loop control system in Fig. 1. The plant is controllable (Dorf & Bishop, 2017) and modeled by the following differential equation of order $n \geq 1$.

$$y^{(n)}(t) + a_{n-1}y^{(n-1)}(t) + \cdots + a_1\dot{y}(t) + a_0 y(t) = b_0 u(t) \tag{2}$$

where $a_0, \ldots, a_{n-1}, b_0 \neq 0 \in \mathbb{R}$ t is the time-independent variable, $u: \mathbb{R}_+ \to \mathbb{R}$ is the time differentiable control signal, and $y: \mathbb{R}_+ \to \mathbb{R}$ is the controlled output. The tracking error, $e: \mathbb{R}_+ \to \mathbb{R}$, is defined as:

$$e(t) = y_r(t) - y(t) \tag{3}$$

With $y_r: \mathbb{R}_+ \to \mathbb{R}$ the reference input.

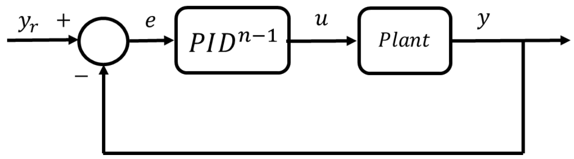

Figure 1. Feedback control system with an n-th order plant and a PID type controller.

Theorem 1: If in the control system of Fig. 1, the plant is modeled by (2) and the reference signal in (3) is constant, then the closed-loop control system can be described in state-variables through the equations:

$$\dot{\boldsymbol{z}}(t) = \boldsymbol{F}\boldsymbol{z}(t) + \boldsymbol{G}\dot{u}(t) \qquad (4)$$

Where:

$$\boldsymbol{F} = \begin{bmatrix} 0 & 1 & 0 & 0 & \dots & 0 \\ 0 & 0 & 1 & 0 & \dots & 0 \\ \vdots & \vdots & \vdots & \vdots & \ddots & \vdots \\ 0 & 0 & 0 & 0 & \dots & 1 \\ 0 & -a_0 & -a_1 & -a_2 & \dots & -a_{n-1} \end{bmatrix}, \boldsymbol{G} = \begin{bmatrix} 0 \\ 0 \\ \vdots \\ 0 \\ -b_0 \end{bmatrix},$$
$$\boldsymbol{z}(t) = [e(t) \quad \dot{e}(t) \quad \dots \quad e^{(n-1)}(t) \quad e^{(n)}(t)]^T$$

Proof: n successive time derivatives of (3) considering a constant reference input yields:

$$\dot{e}(t) = -\dot{y}(t),$$
$$\dot{e}(t) = -\dot{y}(t)$$
$$\vdots$$
$$e^{(n)}(t) = -y^{(n)}(t)$$

Defining state-variables $z_1 = e,\ z_2 = \dot{e}, \dots, z_n = e^{(n)}$ and computing the time derivative of (2) results in:

$$\dot{z}_1 = z_2$$
$$\dot{z}_2 = z_3$$
$$\vdots$$
$$\dot{z}_n = e^{(n+1)} = -y^{(n+1)} = -a_0 z_2 - a_1 z_3 - \dots - a_{n-1} z_n - b_0 \dot{u}$$

This can be rewritten in the form (4) so the theorem is established.

The parameters K_p, $K_i, K_{d_1}, K_{d_2}, \dots, K_{d_{n-1}}$ in (1) must be computed to satisfy desired design requirements for the controlled output $\boldsymbol{y(t)}$. The LQR method is used for this purpose. A quadratic function is defined to have an LQR formulation of the closed-loop system (4).

$$J = \int_0^\infty [\boldsymbol{z}(t)^T \boldsymbol{Q}\boldsymbol{z}(t) + r\dot{u}^2(t)]dt \qquad (5)$$

Where $\boldsymbol{Q}$ is a positive semi-definite matrix that influences the closed-loop transient response.

Remark 1: In general, the purpose of the parameter $r > 0$ within the cost function (5) would be to adjust the amplitude of the derivative of the control signal. However, in this work, it will be seen later that this parameter does not impact the control signal.

It is widely known (Anderson & Moore, 2007) that the state-feedback control law.

$$\dot{u}(t) = -\boldsymbol{k}\boldsymbol{z}(t) \qquad (6)$$

Minimizes (5) and stabilizes (4) when the pair $(\boldsymbol{F}, \boldsymbol{G})$ is controllable. The pair $(\boldsymbol{F}, \boldsymbol{G})$ is controllable if the controllability matrix.

$$\boldsymbol{M_c} = [\boldsymbol{G} \quad \boldsymbol{FG} \quad \boldsymbol{F}^2\boldsymbol{G} \quad \dots \quad \boldsymbol{F}^{n-1}\boldsymbol{G}] \qquad (7)$$

It is nonsingular (Dorf & Bishop, 2017).

Remark 2: The controllability of (4) is necessary because of the LQR problem; therefore, the design of the PID-type controller is constructed from the system (4).

Theorem 2: For the closed-loop system (4), the controllability matrix (7) is nonsingular.

Proof: The determinant of (7) for $\boldsymbol{n \geq 1}$ in (2) can be computed as:

$$\det(\boldsymbol{M_c}) = \begin{cases} -({b_0}^{n+1}), n = 1,4,5,8,9,12,13, \dots \\ {b_0}^{n+1}, n = 2,3,6,7,10,11,14,15, \dots \end{cases}$$

Since b_0 is a real constant different from zero, the pair $(\boldsymbol{F}, \boldsymbol{G})$ is controllable.

Vector $\boldsymbol{k}$ in (6) is given by:

$$\boldsymbol{k} = -r^{-1}\boldsymbol{G}^{\mathbf{T}}\boldsymbol{P} \qquad (8)$$

Where $\boldsymbol{P}$ is a positive definite symmetric matrix solution of the algebraic Riccati equation:

$$\boldsymbol{F}^T\boldsymbol{P} + \boldsymbol{P}\boldsymbol{F} - r^{-1}\boldsymbol{P}\boldsymbol{G}\boldsymbol{G}^T\boldsymbol{P} + \boldsymbol{Q} = \boldsymbol{0} \qquad (9)$$

Equation (6) can be rewritten as:

$$\dot{u}(t) = -\underbrace{[k_1 \quad k_2 \quad \dots \quad k_{n+1}]}_{\boldsymbol{k}} \begin{bmatrix} e(t) \\ \dot{e}(t) \\ \vdots \\ e^{(n)}(t) \end{bmatrix} \qquad (10)$$

Time integration of (10) results in the control policy:

$$u(t) = -k_1 \int_0^t e(\tau)\, d\tau - k_2 e(t) - k_3 \dot{e}(t) - \dots - k_{n+1} e^{(n-1)}(t) \qquad (11)$$

By comparing with (1), the constants of the PID type controller are deduced as:

$$K_i = -k_1, K_p = -k_2, K_{d_1} = -k_3, \dots, K_{d_{n-1}} = -k_{n+1} \quad (12)$$

Expressing $\boldsymbol{P}$ in (8) by:

$$\boldsymbol{P} = \begin{bmatrix} p_{11} & p_{12} & p_{13} & \cdots & p_{1,n+1} \\ p_{12} & p_{22} & p_{23} & \cdots & p_{2,n+1} \\ p_{13} & p_{23} & p_{33} & \cdots & p_{3,n+1} \\ \vdots & \vdots & \vdots & \ddots & \vdots \\ p_{1,n+1} & p_{2,n+1} & p_{3,n+1} & \cdots & p_{n+1,n+1} \end{bmatrix}$$

Allows computing vector $\boldsymbol{k}$ as:

$$\boldsymbol{k} = [k_1 \quad k_2 \quad \dots \quad k_{n+1}] = r^{-1}b_0[p_{1,n+1} \quad p_{2,n+1} \quad \cdots \quad p_{n+1,n+1}] \quad (13)$$

Equation (13) provides a way to connect the solution of the LQR problem with the parameters of the PID type controller (12). Now, in the LQR context, the link with closed-loop dynamics is indirect; it depends on the selection of the matrix $\boldsymbol{Q}$ and the parameter r in (5). Therefore, some trial-and-error procedure is usually necessary to obtain a satisfactory closed-loop response. For this reason, it is interesting to link the LQR problem with the location of poles by requiring that the closed-loop poles of the system (4) with the optimal control policy (12) and (13) be found in some specific region of the complex plane. This work constructs the desired closed-loop polynomial using a dominant pole guarantee criterion (Persson & Åström, 1992). The requirements of the closed-loop control performance in the time domain are converted into a pair of conjugate poles $s_{1,2} = -\alpha \pm j\beta$. Their dominance requires that the ratio of the real part of other poles to $-\alpha$ exceeds λ (λ is usually 3 to 5). Thus, we want all other poles to be at the left of the line $s = -\lambda\alpha$. The desired polynomial is expressed as:

$$(s^2 + 2\zeta\omega_n s + \omega_n{}^2)(s + \lambda\zeta\omega_n)^{n-1} \quad (14)$$

The damping coefficient ζ and the natural frequency ω_n of the dominant poles can be determined in terms of the overshoot OS and the settling time T_s (Dorf & Bishop, 2017).

$$OS = e^{\left(-\zeta\pi/\sqrt{1-\zeta^2}\right)} \Longrightarrow \zeta = 1\Big/\sqrt{1 + \left(\frac{\pi}{ln(M_p)}\right)^2} \quad (15)$$

And:

$$T_s = 4/(\zeta\omega_n) \Longrightarrow \omega_n = 4/\zeta t_s \quad (16)$$

In this way, the desired closed-loop polynomial will meet some temporal design requirements. In this work, once the desired $n+1$ poles have been calculated they will be expressed as $-\mu_1, -\mu_2, \dots, -\mu_{n+1}$, the desired closed-loop polynomial (14) is rewritten as:

$$(s + \mu_1)(s + \mu_2) \dots (s + \mu_{n+1}) \quad (17)$$

Problem 1: Given the system (2). Find the controller parameters in (1) that minimize the quadratic function (5) and satisfy the requirements (15) and (16).

To solve the problem, the closed-loop polynomial of the control system in Fig. 1 is computed using (1). This is:

$$s^{n+1} + \left(a_{n-1} + b_0 K_{d_{n-1}}\right)s^n + \left(a_{n-2} + b_0 K_{d_{n-2}}\right)s^{n-1} + \cdots + \left(a_1 + b_0 K_{d_1}\right)s^2 + \left(a_0 + b_0 K_p\right)s + b_0 K_i \quad (18)$$

By equating the coefficients of the polynomials (17) and (18), equations are found that allow the expression of the elements of the matrix $\boldsymbol{P}$ that appear in (13) in terms of the desired closed-loop poles. Then, by analytically solving (9) using the computed values of $\boldsymbol{P}$, it is possible to determine the elements of the matrix $\boldsymbol{Q} = diag(q_1, \dots, q_{n+1})$. These values now allow us to solve (9) again, and the matrix $\boldsymbol{P}$ that will be obtained produces a vector $\boldsymbol{k}$ in (8) that generates a closed-loop response with zero steady-state error for any constant reference input exhibiting the specifications (15) and (16).

This methodology will be applied to different orders of the model (2).

3. PI tuning method

Direct tuning formulas for the parameters K_p and K_i in (1) will be deduced when $n = 1$ in (2). We have matrices $\boldsymbol{F} = \begin{bmatrix} 0 & 1 \\ 0 & -a_0 \end{bmatrix}$ and $\boldsymbol{G} = \begin{bmatrix} 0 \\ -b_0 \end{bmatrix}$ in (4) for this case. Choosing matrix $\boldsymbol{Q} = \begin{bmatrix} q_1 & 0 \\ 0 & q_2 \end{bmatrix}$ and expressing the positive definite symmetric matrix $\boldsymbol{P}$, solution of (9), as:

$$\boldsymbol{P} = \begin{bmatrix} p_{11} & p_{12} \\ p_{12} & p_{22} \end{bmatrix} \quad (19)$$

Allow us to write (9) as:

$$\begin{bmatrix} 0 & 0 \\ 1 & -a_0 \end{bmatrix}\begin{bmatrix} p_{11} & p_{12} \\ p_{12} & p_{22} \end{bmatrix} + \begin{bmatrix} p_{11} & p_{12} \\ p_{12} & p_{22} \end{bmatrix}\begin{bmatrix} 0 & 1 \\ 1 & -a_0 \end{bmatrix} - r^{-1}\begin{bmatrix} p_{11} & p_{12} \\ p_{12} & p_{22} \end{bmatrix}\begin{bmatrix} 0 \\ -b_0 \end{bmatrix}[0 \quad -b_0]\begin{bmatrix} p_{11} & p_{12} \\ p_{12} & p_{22} \end{bmatrix} + \begin{bmatrix} q_1 & 0 \\ 0 & q_2 \end{bmatrix} = \begin{bmatrix} 0 & 0 \\ 0 & 0 \end{bmatrix}$$

Next some algebra, is obtained the following system of equations:

$$q_1 - r^{-1}b_0{}^2 p_{12}{}^2 = 0$$
$$p_{11} - a_0 p_{12} - r^{-1}b_0{}^2 p_{12}p_{22} = 0$$

$$2p_{12}-2a_0p_{22}-r^{-1}{b_0}^2{p_{22}}^2+q_2=0 \quad (20)$$

The vector $\boldsymbol{k}$ in (13) has the form:

$$\boldsymbol{k}=[k_1 \quad k_2]=\left[-\frac{b_0p_{12}}{r} \quad -\frac{b_0p_{22}}{r}\right] \quad (21)$$

Using (12) and (13), the parameters of the PI controller are calculated as:

$$K_i=\frac{b_0p_{12}}{r},\ K_p=\frac{b_0p_{22}}{r} \quad (22)$$

As (22) depends on p_{12} and p_{22}, only the first and third equations of (20) are necessary.

$$\begin{gathered} q_1-r^{-1}{b_0}^2{p_{12}}^2=0 \\ 2p_{12}-2a_0p_{22}-r^{-1}{b_0}^2{p_{22}}^2+q_2=0 \end{gathered} \quad (23)$$

The characteristic closed-loop polynomial is given by:

$$s^2+\left(b_0K_p+a_0\right)s+K_ib_0 \quad (24)$$

Once the requirements (15) and (16) are converted into a pair of poles $-\mu_1$ and $-\mu_2$. The desired polynomial is:

$$s^2+(\mu_1+\mu_2)s+\mu_1\mu_2 \quad (25)$$

Using (22) and equating (24) and (25) gives:

$$\begin{gathered} p_{12}=\frac{r}{{b_0}^2}(\mu_1\mu_2) \\ p_{22}=\frac{r}{{b_0}^2}(\mu_1+\mu_2-a_0) \end{gathered} \quad (26)$$

Replacing (26) in (23) allows to obtain matrix $\boldsymbol{Q}$ in (5) as:

$$\begin{gathered} q_1=\frac{r}{{b_0}^2}({\mu_1}^2{\mu_2}^2) \\ q_2=\frac{r}{{b_0}^2}({\mu_1}^2+{\mu_2}^2-{a_0}^2) \end{gathered} \quad (27)$$

To verify $\boldsymbol{Q}\geq\boldsymbol{0}$ in (27), it is necessary that $\boldsymbol{\mu_1}^2+\boldsymbol{\mu_2}^2-\boldsymbol{a_0}^2>\boldsymbol{0}$.

4. PID tuning method

Equation (2) now is of order two, and (4) takes the form.

$$\boldsymbol{F}=\begin{bmatrix}0 & 1 & 0\\ 0 & 0 & 1\\ 0 & -a_0 & -a_1\end{bmatrix},\boldsymbol{G}=\begin{bmatrix}0\\ 0\\ -b_0\end{bmatrix},\boldsymbol{z}=\begin{bmatrix}e(t)\\ \dot{e}(t)\\ \ddot{e}(t)\end{bmatrix} \quad (28)$$

The matrix $\boldsymbol{P}=\boldsymbol{P}^T>0$ solution of (9) is expressed as:

$$\boldsymbol{P}=\begin{bmatrix}p_{11} & p_{12} & p_{13}\\ p_{12} & p_{22} & p_{23}\\ p_{13} & p_{23} & p_{33}\end{bmatrix} \quad (29)$$

After using $\boldsymbol{Q}=diag(q_1,q_2,q_3)$ in the Ricatti equation (9), it is obtained the system of equations:

$$-r^{-1}{b_0}^2{p_{13}}^2+q_1=0 \quad (30)$$

$$p_{11}-a_0p_{13}-r^{-1}{b_0}^2p_{13}p_{23}=0 \quad (31)$$

$$p_{12}-a_1p_{13}-r^{-1}{b_0}^2p_{13}p_{33}=0 \quad (32)$$

$$2p_{12}-2a_0p_{23}-r^{-1}{b_0}^2{p_{23}}^2+q_2=0 \quad (33)$$

$$p_{13}+p_{22}-a_1p_{23}-a_0p_{33}-r^{-1}{b_0}^2p_{23}p_{33}=0 \quad (34)$$

$$2p_{23}-2a_1p_{33}-r^{-1}{b_0}^2{p_{33}}^2+q_3=0 \quad (35)$$

The control policy (11) using the solution of (9) is expressed as:

$$u(t)=-\left[\frac{b_0p_{13}}{r} \quad \frac{b_0p_{23}}{r} \quad \frac{b_0p_{33}}{r}\right]\begin{bmatrix}\int_0^t e(\tau)\,d\tau\\ e(t)\\ \dot{e}(t)\end{bmatrix} \quad (36)$$

Hence, the PID constants are obtained through:

$$K_i=\frac{b_0p_{13}}{r},K_p=\frac{b_0p_{23}}{r},K_d=\frac{b_0p_{33}}{r} \quad (37)$$

This implies that the equations (30-35) must be solved for $p_{13},p_{23,}$ and p_{33}. This is achieved by isolating p_{12} in (32) and replacing it in (33). The resulting equations used for designing the PID controller are:

$$\begin{gathered} -r^{-1}{b_0}^2{p_{13}}^2+q_1=0 \\ 2a_1p_{13}+2r^{-1}{b_0}^2p_{13}p_{33} \\ -2a_0p_{23}-r^{-1}{b_0}^2{p_{23}}^2+q_2=0 \\ 2p_{23}-2a_1p_{33}-r^{-1}{b_0}^2{p_{33}}^2+q_3=0 \end{gathered} \quad (38)$$

The closed-loop polynomial is given by:

$$s^3+(b_0K_d+a_1)s^2+\left(b_0K_p+a_0\right)s+K_ib_0 \quad (39)$$

After transforming the time requirements into three poles $\{-\mu_1-,\mu_2,-\mu_3\}$ (a fast pole has been included). The desired closed-loop polynomial is written as:

$$s^3+(\mu_1+\mu_2+\mu_3)s^2+(\mu_1\mu_2+\mu_1\mu_3+\mu_2\mu_3)s+\mu_1\mu_2\mu_3 \quad (40)$$

Using (37) and equating coefficients in (39) and (40) results in:

$$p_{13} = \frac{r\mu_1\mu_2\mu_3}{{b_0}^2}$$
$$p_{23} = \frac{r}{{b_0}^2}(\mu_1\mu_2 + \mu_1\mu_3 + \mu_2\mu_3 - a_0)$$
$$p_{33} = \frac{r}{{b_0}^2}(\mu_1 + \mu_2 + \mu_3 - a_1) \quad (41)$$

Replacing (41) in (38) allows us to obtain the result:

$$q_1 = \frac{r{\mu_1}^2{\mu_2}^2{\mu_3}^2}{{b_0}^2}$$
$$q_2 = \frac{r}{{b_0}^2}({\mu_1}^2{\mu_2}^2 + {\mu_1}^2{\mu_3}^2 + {\mu_2}^2{\mu_3}^2 - {a_0}^2)$$
$$q_3 = \frac{r}{{b_0}^2}({\mu_1}^2 + {\mu_2}^2 + {\mu_3}^2 + 2a_0 - {a_1}^2) \quad (42)$$

To verify $\boldsymbol{Q} \geq 0$ in (42), it is necessary that ${\mu_1}^2{\mu_2}^2 + {\mu_1}^2{\mu_3}^2 + {\mu_2}^2{\mu_3}^2 - {a_0}^2 > 0$ and ${\mu_1}^2 + {\mu_2}^2 + {\mu_3}^2 + 2a_0 - {a_1}^2 > 0$.

5. High-order systems

This section shows the results of extending the procedure for high-order systems. For example, if $n = 3$ in (2), the PID^2 controller (1) will have the form:

$$u(t) = K_p e(t) + K_i \int_0^t e(\tau)\, d\tau + K_{d_1}\dot{e}(t) + K_{d_2}\ddot{e}(t)$$

In this case, there would be four parameters to adjust $(K_p, K_i, K_{d_1}, K_{d_2})$. The four elements of matrix $\boldsymbol{Q} = \boldsymbol{diag}(q_1, q_2, q_3, q_4)$ in terms of the desired closed-loop poles can be computed as:

$$q_1 = \frac{r{\mu_1}^2{\mu_2}^2{\mu_3}^2{\mu_4}^2}{{b_0}^2} \quad (43)$$

$$q_2 = \frac{r}{{b_0}^2}({\mu_1}^2{\mu_2}^2{\mu_3}^2 + {\mu_1}^2{\mu_2}^2{\mu_4}^2 + {\mu_1}^2{\mu_3}^2{\mu_4}^2 + {\mu_2}^2{\mu_3}^2{\mu_4}^2 - {a_0}^2)$$
$$q_3 = \frac{r}{{b_0}^2}({\mu_1}^2{\mu_2}^2 + {\mu_1}^2{\mu_3}^2 + {\mu_1}^2{\mu_4}^2 + {\mu_2}^2{\mu_3}^2 + {\mu_2}^2{\mu_4}^2 + {\mu_3}^2{\mu_4}^2 - {a_1}^2 + 2a_0a_2)$$
$$q_4 = \frac{r}{{b_0}^2}({\mu_1}^2 + {\mu_2}^2 + {\mu_3}^2 + {\mu_4}^2 + 2a_1 - {a_2}^2)$$

And if $n = 4$ in (2), the following values of the matrix $\boldsymbol{Q}$ allow optimal tuning of the five parameters of the PID^3 $(K_p, K_i, K_{d_1}, K_{d_2}, K_{d_3})$ controller:

$$q_1 = \frac{r{\mu_1}^2{\mu_2}^2{\mu_3}^2{\mu_4}^2{\mu_5}^2}{{b_0}^2}$$
$$q_2 = \frac{r}{{b_0}^2}({\mu_1}^2{\mu_2}^2{\mu_3}^2{\mu_4}^2 + {\mu_1}^2{\mu_2}^2{\mu_3}^2{\mu_5}^2 + {\mu_1}^2{\mu_2}^2{\mu_4}^2{\mu_5}^2 + {\mu_1}^2{\mu_3}^2{\mu_4}^2{\mu_5}^2 + {\mu_2}^2{\mu_3}^2{\mu_4}^2{\mu_5}^2 - {a_0}^2)$$
$$q_3 = \frac{r}{{b_0}^2}({\mu_1}^2{\mu_2}^2{\mu_3}^2 + {\mu_1}^2{\mu_2}^2{\mu_4}^2 + {\mu_1}^2{\mu_2}^2{\mu_5}^2 + {\mu_1}^2{\mu_3}^2{\mu_4}^2 + {\mu_1}^2{\mu_3}^2{\mu_5}^2 + {\mu_1}^2{\mu_4}^2{\mu_5}^2 + {\mu_2}^2{\mu_3}^2{\mu_4}^2 + {\mu_2}^2{\mu_3}^2{\mu_5}^2 + {\mu_2}^2{\mu_4}^2{\mu_5}^2 + {\mu_3}^2{\mu_4}^2{\mu_5}^2 - {a_1}^2 + 2a_3 + 2a_0a_2)$$
$$q_4 = \frac{r}{{b_0}^2}({\mu_1}^2{\mu_2}^2 + {\mu_1}^2{\mu_3}^2 + {\mu_1}^2{\mu_4}^2 + {\mu_1}^2{\mu_5}^2 + {\mu_2}^2{\mu_3}^2 + {\mu_2}^2{\mu_4}^2 + {\mu_2}^2{\mu_5}^2 + {\mu_3}^2{\mu_4}^2 + {\mu_3}^2{\mu_5}^2 + {\mu_4}^2{\mu_5}^2 - {a_2}^2 + 2a_0 + 2a_1a_3)$$
$$q_5 = \frac{r}{{b_0}^2}({\mu_1}^2 + {\mu_2}^2 + {\mu_3}^2 + {\mu_4}^2 + {\mu_5}^2 + 2a_2 - {a_3}^2) \quad (44)$$

To verify $\boldsymbol{Q} \geq 0$ in (43) and (44), some apparent conditions would have to be imposed. But in this case, a higher order makes it more complex to verify them by imposing a dominant pole guarantee criterion where there are some conjugate complex poles. That is why, to satisfy the conditions, sometimes it is recommended to use desired poles of real value.

6. PID^{n-1} design

A legitimate question is what to do with r in (5). The LQR control theory establishes that this parameter regulates the control effort. However, in this work, it has no influence. This term disappears when the controller equations are formed to calculate the gains in (1). For example, when (26) is replaced in (22), the parameter r is canceled. So, we set the value $r = 1$ in all the calculations.

For ease of reference, Table 1 summarizes the procedure for computing the gains of the PI controller. Replacing the equations and adjusting Table 1 to design the other PID-type controllers is straightforward.

Table 1. The procedure for computing the PI controller gains.

Input	Plant model (1), and desired OS and T_s
Step 1	Construct the augmented tracking system (4) to compute the matrices $\boldsymbol{F}$ and $\boldsymbol{G}$
Step 2	Use (15) and (16) and the dominant pole guarantee criterion to obtain the desired poles $P = [-\mu_1, -\mu_2]$
Step 3	Obtain the weighting matrix $\boldsymbol{Q}$ by using (27)
Step 4	Solve the LQR problem (5) through the Matlab command. $\gg K = lqr(F, G, Q, r) < enter >$
Output	Using (12), calculate the PI controller gains from the vector K as $[K_i \quad K_p] = [-K(1), -K(2)]$

The pure derivative terms in (1) are not implemented directly to avoid sudden variations in the control signal, a situation known as the "derivative kick," and the undesirable noise amplification. It is usually cascaded by a first-order low-pass filter (parameter N_1) (Atherton & Majhi, 1999).

$$G_{PID}(s) = K_p + \frac{K_i}{s} + \frac{K_{d_1}N_1}{1 + \frac{N_1}{s}} \quad (45)$$

In this work, we adopt and extend this idea. Thus, the implementation of the general derivative term $K_{d_{n-1}} e^{(n-1)}(t)$ is shown in Fig. 2.

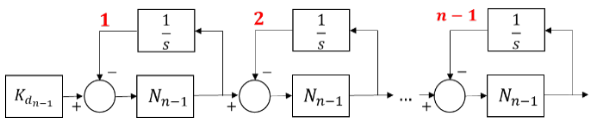

Figure 2. Low-pass Implementation of the derivative terms in the PID^{n-1} controller

7. Numerical results

PI, PID, and PID^2 controllers are implemented for plants of order 1, 2, and 3, respectively.

7.1. Heat flow experiment (n=1)

The heat flow experiment (HFE) has been developed by Quanser Innovative Edutech2012) to support the study of heat transmission in a fiberglass duct; and the control of the temperature at different points where some sensors have been placed. It is a very convenient process for learning fluid dynamics and thermodynamics phenomena and validating temperature control strategies (Orman, 2019, 2022; Jovanović & Zarić, 2022). The mathematical model of the EFC is given by the transfer function (Al-Saggaf et al., 2016):

$$\frac{Y(s)}{U(s)} = \frac{0.148}{s+0.033} e^{-0.3s} \tag{46}$$

The controlled output $y(t)$ is the temperature measured by sensor 1 (closest to the heating element), and the control input is the heating voltage restricted to the interval $[0-12]$ V. The simulations of the closed-loop control system are implemented using equation (46), but the augmented system (4), employed for the PI controller design, is constructed from the rational part of (46) and takes the form:

$$\boldsymbol{F} = \begin{bmatrix} 0 & 1 \\ 0 & -0.033 \end{bmatrix}, \boldsymbol{G} = \begin{bmatrix} 0 \\ -0.148 \end{bmatrix}$$

The specifications for this system are $OS \leq 10\ \%$ and $T_s \leq 60$ s. Table 2 depicts the results obtained following the procedure of Table 1 for an overshoot of 1 % and settling times of 20, 40, and 60 s.

Table 2. PI gains for $OS = 1\%$, and $T_s = 20, 40, 60$ s.

	$OS = 0.01$		
	$T_s = 60$ s	$T_s = 40$ s	$T_s = 20$ s
Q	$\begin{bmatrix} 0.002 & 0 \\ 0 & 0.167 \end{bmatrix}$	$\begin{bmatrix} 0.010 & 0 \\ 0 & 0.438 \end{bmatrix}$	$\begin{bmatrix} 0.157 & 0 \\ 0 & 1.903 \end{bmatrix}$
K_i	0.0440	0.0990	0.3960
K_p	0.6779	1.1284	2.4797

Fig. 3 shows the tracking of the controlled output when a variable temperature profile is applied in the input reference, and Fig. 4 shows the corresponding heating voltage. The results of this test are entirely satisfactory, although it should be noted that as the T_s condition is more demanding, the control signal leaves the actuator range for a short time.

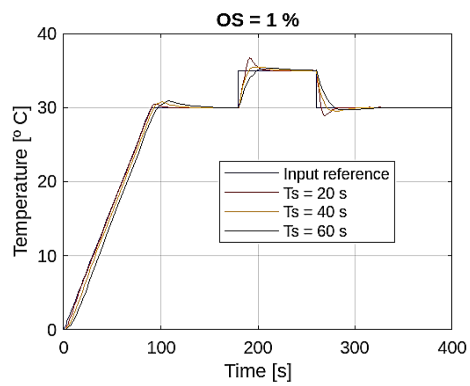

Figure 3. Controlled output and input reference for the HFE considering different values of settling time and a fixed overshoot of 1 %.

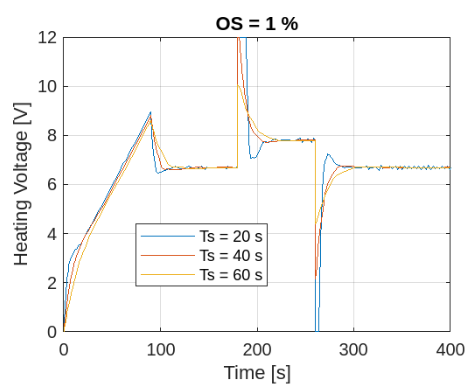

Figure 4. Heating voltage input for the HFE considering different values of settling time and a fixed overshoot of 1 %.

7.2. Coupled tank system (n=2)

The coupled tank system consists of a single pump with two tanks. Each tank is equipped with a pressure sensor to measure the water level. The pump drives water from the bottom reservoir to the system's top. The state-space nonlinear model of the coupled tank system is presented in (47) (Teppa-Garran & El Gharib, 2024). Here, the control signal u corresponds to the input voltage applied to the pump restricted to be in the interval $[0-22]$ V, x_1 and x_2 are tank 1 and 2 levels varying within $[0-30]$ cm. The output y is the level of the second tank.

$$\begin{aligned} \dot{x}_1(t) &= -0.904\sqrt{x_1(t)} + 0.258u(t) \\ \dot{x}_2(t) &= 0.904\sqrt{x_1(t)} - 0.508\sqrt{x_2(t)} \\ y(t) &= x_2(t) \end{aligned} \tag{47}$$

Linearizing (47) in the operation point $(15, 15)$ cm, gives the transfer function

$$\frac{Y(s)}{U(s)} = \frac{0.0302}{s^2+0.183s+0.0077} \tag{48}$$

From (48) is built the augmented system (4) for PID controller design as:

$$\boldsymbol{F} = \begin{bmatrix} 0 & 1 & 0 \\ 0 & 0 & 1 \\ 0 & -0.0077 & -0.183 \end{bmatrix}, \boldsymbol{G} = \begin{bmatrix} 0 \\ 0 \\ -0.0302 \end{bmatrix}$$

The time requirements are $OS \leq 10~\%$ and $T_s \leq 90$ s. It is selected $OS = 4~\%$ and $T_s = 50$ s in (15) and (16) to give through (42):

$$\boldsymbol{Q} = \begin{bmatrix} 0.0274 & 0 & 0 \\ 0 & 0.2127 & 0 \\ 0 & 0 & 156.2632 \end{bmatrix}$$

Solving the *lqr* problem with *Matlab* results in:

$$[K_i \quad K_p \quad K_{d_1}] = [0.1655 \quad 2.2780 \quad 12.4834].$$

The parameter N_1 in (45) uses the value $N_1 = 10$ (Xue et al., 2002). The simulation considers the nonlinear model of the coupled tank system (47) and the presence of a band-limited white noise signal of power 5 % in the feedback loop. The performance of the optimal PID is compared with that of traditional PID tuning using the Chien-Hrones-Reswick rule. Figure 5 displays the tracking of the second tank level, and Figure 6 shows the control voltage pump.

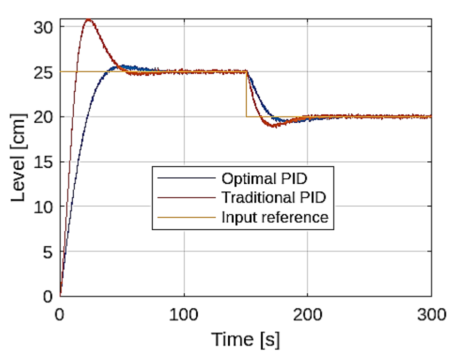

Figure 5. Second tank level and input reference for the coupled tank system.

7.3. Radar antenna ($n = 3$)

The process is modeled by two inertias linked together by a spring. The input is the motor voltage constraint to $[-5, 5]$ V, and the output is the position. The transfer function (Hamamci et al., 2002) is given by:

$$\frac{Y(s)}{U(s)} = \frac{0.1}{s^3+0.6s^2+0.1s} \tag{49}$$

The augmented system (4) is:

$$\boldsymbol{F} = \begin{bmatrix} 0 & 1 & 0 & 0 \\ 0 & 0 & 1 & 0 \\ 0 & 0 & 0 & 1 \\ 0 & 0 & -0.1 & -0.6 \end{bmatrix}, \boldsymbol{G} = \begin{bmatrix} 0 \\ 0 \\ 0 \\ -0.1 \end{bmatrix}$$

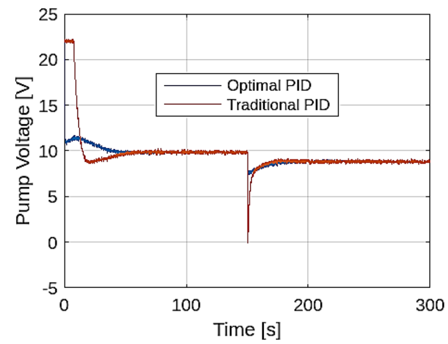

Figure 6. Pump voltage for the coupled tank system.

$$\boldsymbol{Q} = \begin{bmatrix} 0.7054 & 0 & 0 & 0 \\ 0 & 0.6129 & 0 & 0 \\ 0 & 0 & 98.1094 & 0 \\ 0 & 0 & 0 & 183.2020 \end{bmatrix}$$

Solving the *lqr* problem with *Matlab* results in:

$$[K_i \quad K_p \quad K_{d_1} \quad K_{d_2}] = [0.840 \quad 5.680 \quad 17.840 \quad 18]$$

The PID^2 is implemented as:

$$G_{PID^2}(s) = K_p + \frac{K_i}{s} + \frac{K_{d_1}N_1}{1+\frac{N_1}{s}} + \frac{K_{d_2}{N_2}^2}{\left(1+\frac{N_2}{s}\right)^2}$$

With $N_1 = N_2 = 10$. In Fig.7, the position output can be seen when a unit step reference input is applied; Fig. 8 shows the control signal for this case. The tracking is satisfactory, and the control signal is within the physical limits of the motor. Some problems appear when the feedback loop includes a noise signal of power 5 %. Figure 9 shows the control signal for this situation.

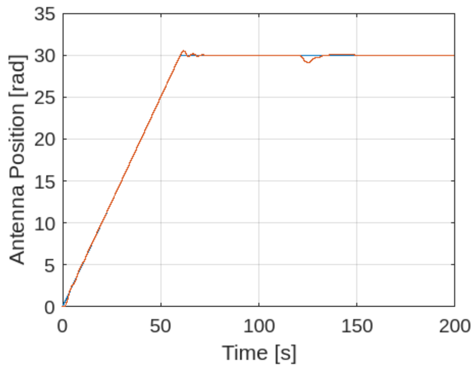

Figure 7. Position response of the radar antenna.

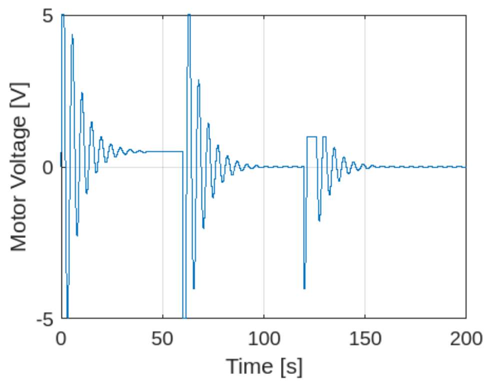

Figure 8. The control signal of the radar antenna.

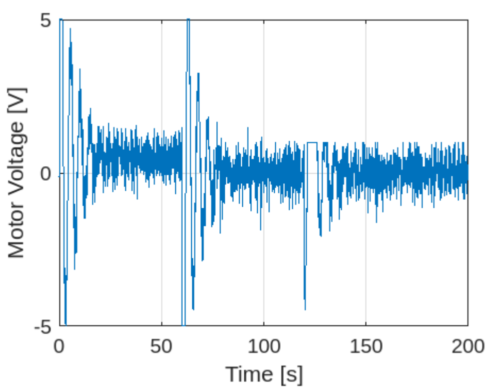

Figure 9. Control signal considering a noise signal in the feedback loop.

8. Discussion and conclusions

Direct design methods for optimal tuning of a PID-type controller have been developed using the results of LQR optimal control theory. The desired time requirements of the controlled closed-loop response in terms of overshoot, settling time, and zero tracking error of constant reference inputs are defined through the matrix $\boldsymbol{Q}$ of the quadratic function of the LQR problem. In this way, the feedback gain vector, the solution of the Riccati equation of the LQR problem, can be connected with the parameters of the controllers. Then, using the PID-type controller, the control system will exhibit the desired time specifications in its closed-loop response.

The parameter r in the quadratic function of the LQR problem has no impact on the amplitude of the control signal for the proposed design method. The control effort can only be regulated through time dynamic specifications, making them more or less demanding to have an indirect mechanism of influence on the control signal. On the other hand, pure derivative terms cannot be implemented directly in the control loop to avoid problems arising in instantaneous changes of the reference input, measurement noise, and eventual loss of stability.

Conflict of interest

The authors have no conflict of interest to declare.

Acknowledgments

The authors are grateful for the support provided by the Research Program of the Metropolitan University in Caracas, Venezuela, through project number PI-B-02-23-24.

Funding

The authors received no specific funding for this work.

References

Anh, N. T. (2020). Control an active suspension system by using PID and LQR controller. *International Journal of Mechanical and Production Engineering Research and Development*, *10*(3), 7003-7012.

Al-Saggaf, U., Mehedi, I., Bettayeb, M., & Mansouri, R. (2016). Fractional-order controller design for a heat flow process. *Proceedings of the Institution of Mechanical Engineers, Part I: Journal of Systems and Control Engineering*, *230*(7), 680-691. https://doi.org/10.1177/0959651816649917

Anderson, B. D., & Moore, J. B. (2007). *Optimal control: linear quadratic methods*. Courier Corporation.

Argentim, L. M., Rezende, W. C., Santos, P. E., & Aguiar, R. A. (2013). PID, LQR and LQR-PID on a quadcopter platform. In *2013 International Conference on Informatics, Electronics and Vision (ICIEV)* (pp. 1-6). IEEE.

Astrom, K. J. & Hagglund, T. (1995). PID controllers: theory, design, and tuning. *The International Society of Measurement and Control*.

Atherton, D. P., & Majhi, S. (1999). Limitations of PID controllers. In *Proceedings of the 1999 American Control Conference (Cat. No. 99CH36251)* (Vol. 6, pp. 3843-3847). IEEE. https://doi.org/10.1109/ACC.1999.786236

Choubey, C., & Ohri, J. (2022). Tuning of LQR-PID controller to control parallel manipulator. *Neural Computing and Applications*, *34*(4), 3283-3297. https://doi.org/10.1007/s00521-021-06608-0

Desborough, L. & Miller, R. (2002). Increasing customer value of industrial control performance monitoring-Honeywell's experience. In *AIChE symposium series* (No. 326, pp. 169-189). New York; American Institute of Chemical Engineers; 1998.

Dorf, R. & Bishop, R. (2017). Modern control systems. Pearson Prentice Hall.

Hamamci, S., Koksal, M. & Manabe, S. (2002). Robust position control of a radar antenna with the coefficient diagram method. In *The 4th Asian Control Conf., 2002*.

He, J. B., Wang, Q. G., & Lee, T. H. (2000). PI/PID controller tuning via LQR approach. *Chemical Engineering Science*, *55*(13), 2429-2439. https://doi.org/10.1016/S0009-2509(99)00512-6

Heidari, A. H., Etedali, S., & Javaheri-Tafti, M. R. (2018). A hybrid LQR-PID control design for seismic control of buildings equipped with ATMD. *Frontiers of Structural and Civil Engineering*, *12*, 44-57. https://doi.org/10.1007/s11709-016-0382-6

Jovanović, R., & Zarić, V. (2022). Identification and control of a heat flow system based on the Takagi-Sugeno fuzzy model using the grey wolf optimizer. *Thermal Science*, *26*(3), 2275-2286. https://doi.org/10.2298/TSCI210825324

Lavretsky, E., Wise, K.A. (2013). Optimal Control and the Linear Quadratic Regulator. In: Robust and Adaptive Control. Advanced Textbooks in Control and Signal Processing. Springer, London. https://doi.org/10.1007/978-1-4471-4396-3_2

Lee, J., Cho, W., & Edgar, T. F. (2014). Simple analytic PID controller tuning rules revisited. *Industrial & Engineering Chemistry Research*, *53*(13), 5038-5047.

Oral, Ö., Çetin, L., & Uyar, E. (2010). A Novel Method on Selection of Q And R Matrices In The Theory Of Optimal Control. *International Journal of Systems Control*, *1*(2).

Orman, K. (2019). Temperature profile tracking control with memristor based PI controller in the heat flow system. *Int. J. Mod. Res. Eng. Technol*, *4*, 12-15.

Orman, K. (2022). Design of a memristor-based 2-DOF PI controller and testing of its temperature profile tracking in a heat flow system. *IEEE Access*, *10*, 98384-98390. https://doi.org/10.1109/ACCESS.2022.3206022

Persson, P., & Åström, K. J. (1992). Dominant pole design-a unified view of PID controller tuning. *IFAC Proceedings Volumes*, *25*(14), 377-382. https://doi.org/10.1016/S1474-6670(17)50763-6

Quanser, Q. (2012). Innovative Edutech-Heat Flow Laboratory. *Quanser Inc., Markham, Canada*.

Teppa-Garran, P. A., & Garcia, G. (2013). Optimal tuning of PI/PID/PID (n-1) controllers in active disturbance rejection control. *Journal of Control Engineering and Applied Informatics*, *15*(4), 26-36.

Teppa-Garran, P., & Garcia, G. (2014). ADRC tuning employing the LQR approach for decoupling uncertain MIMO systems. *Information Technology and Control*, *43*(2), 157-165. https://doi.org/10.5755/j01.itc.43.2.4059

Teppa-Garran, P., Arzola, F., & Elyas, E. (2021). Ajuste óptimo de controladores PID mediante Matlab/Simulink. *Anales de Ciencias Básicas, Físicas y Naturales*, (37), 15-32. https://doi.org/10.58479/acbfn.2021.20

Teppa-Garran, P. & El Gharib, G. (2024). Computer-assisted optimal tuning of PI controllers for nonlinear systems with amplitude constraints on the actuator, *Ciencia e Ingeniería*, *45*(1), 1-10.

Xue, D., Chen, Y., & Atherton, D. P. (2007). *Linear feedback control: analysis and design with MATLAB*. Society for Industrial and Applied Mathematics.